Atmospheric Singular Vectors and Teleconnections

A.Will, U.Harlander and W.Metz

Zusammenfassung

Bekanntlich sind atmosphärische Rossbywellezüge (RWTs) Lösungen der Singular Vector Analyse eines gedämpften, barotropen Modells mit Nordwinter Grundströmen. In den SV Basen der verwendeten 40 DJF Grundströme konnten nur wenige wachsende den Rossbywellenzügen ähnliche (RWT Moden) Singulären Vektoren (SVen) gefunden werden. Die RWT Moden kommen nur in einigen wenigen Gebieten der Erde vor. Die instabilste Mode entwickelt sich in der Region des Nordpazifiks (NPACs) innerhalb von 4 Tagen in jedem der verwendeten beobachteten DJF Grundstöme. Alle anderen RWT Moden kommen nur bei Verwendung einiger der Grundströme vor. Ihre Entwicklungspfade sind eindeutig für Entwicklungszeiten bis zu 96h und streuen für längere Zeiten. Die NPAC Mode erklärt zum Optimierungszeitpunkt 96h bis zu 60% der atmosphärischen kinetischen Energie (KE) auf der 300 hPa Fläche in der NPAC Region. Es konnte auch gezeigt werden, daß die Zeitreihe des beobachteten Wachstums der NPAC Mode mit dem berechneten Wachstum (den Eigenwerten) konsistent ist. Interessanterweise zeigt die NPAC-KE zum Optimierungszeitpunkt 96h auch eine schwach signifikante Korrelation mit dem PNA-Index, die für die Optimierungszeit 144h nicht mehr exisitiert.
Die Ergebnisse legen die Vermutung nahe, daß die verwendeten Grundströme die Entwicklung der RWT Moden bis zu einer Entwicklungszeit von 4 Tagen dominieren und daß die finite Instabilität maßgelich zur Entwicklung der beobachteten NPAC Rossbywellenzügen in der Atmosphäre beiträgt. Die Ergebnisse geben Hinweise darauf, daß die NPAC mode auch einen Beitrag zur Entwicklung der PNA leistet.

Abstract

Atmospheric Rossby wave trains (RWTs) are known to be solutions of Singular Vector (SV) analysis of a damped barotropic model with northern winter basic flows. Using 40 DJF basic flows growing RWT like SVs (RWT modes) can be found in some regions of the globe only. The most instable RWT mode develops in the North-Pacific (NPAC) region (within 4 days) in each of the observed DJF basic flows considered. All the other RWT modes are SVs for some of the basic flows only. They have remarkably propagation paths for development times up to 96h and spread for longer times.
The NPAC modes at optimization time of 96h explain up to 60 % of the atmospheric kinetic energy (KE) at 300 hPa in the NPAC region. Moreover, the observed growth of the NPAC mode is consistent with the calculated growth (eigen values). Furthermore, the NPAC-KE at optimization time $t_{opt} = 96$h exhibits a weakly significant correlation with the PNA-Index. No such correlation could be found for $t_{opt} = 144$h
The results indicate that the basic flows considered dominate the development of RWT

modes up to 96 h and that SVs significantly contribute to the observed NPAC RWT. They give some hints for a possible connection between the NPAC mode and the famous PNA-teleconnection.

1 Introduction

After more than 20 years of discussion there ,,is still no convincing comprehensive dynamical explanation for the teleconnection patterns" (*Navarra*, 1995), which are characterized by covariance on large space scales and time scales beyond the weather. The discussion is still rather broad and spans from the excitation of Rossby wave trains (RWTs) by local orographic and thermal forcing (*Hoskins and Karoly*, 1981) to RWT propagation in zonally asymmetric basic flows (*Simmons et al.*, 1983; *Hoskins and Ambrizzi*, 1997; *Branstator*, 2002). For the latter, possible mechanism are barotropic and baroclinic instability, non-modal growth of Neutral Vectors (*Metz*, 1994; *Goodman and Marshall*, 2002) and Singular Vectors (SVs) (*Li and Ji*, 1997). The SVs can be characterized as optimally growing perturbations in a finite time interval. It has been shown that the finite time instability can explain the occurence of dominant "modes" in stable flows. I.e., even under realistic damping the SVs exhibit reasonable growth factors within some days (*Borges and Sardeshmukh*, 1995).

As pointed out by *Buizza and Palmer* (1995) and stated by *Hoskins et al.* (2000), RWTs are closely related to SVs. Together with the fact that RWTs are also important for the organization of teleconnections it appears obvious to connect both. *Li and Ji* (1997) tried to establish a relation between SVs and RWTs using a climatological basic flow. They calculated optimally forced SVs of a climatological basic flow computed from DJF 1980-1989 assuming the energy of the perturbation at initial time to be zero. The two leading forced SVs of their analysis exhibit the structure of a local RWT similar to the leading SVs of the unforced equation with a shape similar to the east Asia-Pacific pattern.

The relevance of finite time instability for teleconnections is still under discussion. *Sardeshmukh et al.* (1997) concluded that the framework of unforced barotropic model is insufficient and the knowledge of forcing is needed to address this question. However, the global energy and the energy in a limited region are not necessarily correlated. Furthermore, as will be discussed in more detail, the development of the shape of some RWT like SVs is dominated by the basic flow. In order to further investigate the relevance of SVs for atmospheric dynamics and for the occurence of teleconnections we analysed the space-time structure of the observed kinetic energy in terms of SVs in regions of interest. Hereby we focused our attention on the RWT modes.

In section 2 we outline the formalism of SV analysis and introduce variables used later. In section 3 we address the question of interannual variability of non-forced SVs growing in a seasonally averaged flow. We further investigate to which extend the SVs calculated can be found in observations. We finally ask, whether the leading SVs are related to the PNA.

2 Model and Method

The model used is the linearised damped non-forced 2D vorticity equation with the same model parameters as in *Li and Ji* (1997). Due to the linear damping used (= 1/7d) (*Lau*, 1979) all basic flows used are barotropically stable. The model is solved in spectral space using a T21 truncation. The solution of the 480 dimensional models perturbation equation is given by

$$\mathbf{\Psi}(t) = \mathbb{P}(t)\mathbf{\Psi}(0) \tag{1}$$

were $\mathbf{\Psi}$ denote the streamfunction. The linear operator $\mathbb{P}(t)$ depends on the basic flow chosen and is called propagator.

SVs (see *Buizza and Palmer*, 1995; *Li and Ji*, 1997, for details) are those solutions of the models equation which maximize energy at $t = t_{opt}$. The kinetic energy norm $||\cdot||_E$ is given as

$$||\mathbf{\Psi}||_E^2 = (\mathbf{\Psi}, \mathbf{\Psi})_E = \mathbf{\Psi}^T \mathbb{D}\, \mathbf{\Psi}. \tag{2}$$

where $(\cdot,\cdot)_E$ is the "energy" scalar product. The diagonal matrix $\mathbb{D}$ contains the coefficients $n(n+1)$, where n is the total wavenumber (see *Heinrich*, 1999, for details). Assuming the energy at initial time $||\mathbf{\Psi}(0)||_E^2 = 1$, the optimization problem leads to the following eigenvalue equation:

$$(\mathbb{P}^T(t_{opt})\mathbb{D}\mathbb{P}(t_{opt}) - \sigma_k^2\mathbb{D})\mathbf{s_k}(0) = 0. \tag{3}$$

Inserting the eigenvectors $\mathbf{s}_k(0)$ in (1) the SVs $\mathbf{s}_k(t)$ at different development times t can be calculated. The non-negative real eigenvalues $\sigma_k^2 = ||\mathbf{s}_k(t_{opt})||_E^2 / ||\mathbf{s}_k(0)||_E^2$ give the growth of kinetic energy of the SVs between $t = 0$h and $t = t_{opt}$. They are ranked in terms of magnitude (i.e., the first SV has maximal energy growth). The SVs $\mathbf{s}_k(0,j)$ and $\mathbf{s}_k(t_{opt},j)$. form a complete orthonomal basis for $t = 0$ and a complete orthogonal basis for $t = t_{opt}$ for each basic flow.
The basic flows are derived from 0h streamfunction reanalysis data $\mathbf{\Psi}(i,j)$ on the 300 hPa level. Here j denotes the seasons DJF 58/59 ($j = 58$) to DJF 97/98 ($j = 97$) and i the 90 days in each season. We denote the seasonal DJF average as $\widetilde{\mathbf{\Psi}}(j)$ and the climatological average over all 40 seasons as $\overline{\mathbf{\Psi}}$.

Using (1) we can calculate the development of any initial perturbation $\mathbf{\Psi}(0)$ in space and time. Inserting a basis vector $\mathbf{s}_k(0,l)$ in (1) and using a propagator $\mathbb{P}_j(t)$ from season j we get the development of the SV of season l in season j ($\mathbf{r}_{k,l}(t,j) = \mathbb{P}_j(t)\mathbf{s}_k(0,l)$). In general, the structure $\mathbf{r}_{k,l}(t,j)$ is a mixture of SVs $\mathbf{s}_k(t,l)$. Now a time series of growth factors for each $\mathbf{r}_{k,l}(t,j)$ may be calculated. The growth factor is a time dependent quantity similar to the eigenvalue, but uniquely related to a specific SV:

$$g_{k,l}(j) = \frac{||\mathbf{r}_{k,l}(t_{opt},j)||_E^2}{||\mathbf{s}_k(0,l)||_E^2} \tag{4}$$

$g_{k,l}(j)$ is the growth factor of the k-th SV of the basic flow l developing in the basic flow of year j, in contrast to the eigenvalue $\sigma_k^2(j)$, which is the growth factor of the k-th SV of the basic flow j.
In addition to the growth factors we introduce the quantities

$$a_{k,l}(i,j) = (\mathbf{\Psi}(i,j), \frac{1}{\sigma_k^2(l)}\mathbf{s}_k(t_{opt},l))_E \tag{5}$$

and

$$b_{k,l}(i,j)) = (\mathbf{\Psi}(i,j), \mathbf{s}_k(0,l))_E, \tag{6}$$

which are the projection amplitudes relative to the energy scalar product (2) of NCEP data (*Kalnay et al.*, 1996) on SVs at optimization and at initial time for DJF basic state flow l. The total kinetic energy is then given by the sum of squared projection amplitudes

$$E(i,j) = \sum_{k=1}^{N} a_{k,l}^2(i,j) = \sum_{k=1}^{N} b_{k,l}^2(i,j). \tag{7}$$

Of course, the squared projection amplitudes $a_{k,l}^2(i,j)$ and $b_{k,l}^2(i,j)$ are very different in general and give the fraction of total kinetic energy explained by the k-th SV in observed data at $t = t_{opt}$ and $t = 0$, respectively.

For the analysis of the observed NPAC mode we introduce streamfunction fields $\mathbf{\Psi}_{NPAC}(i,j)$ and $\mathbf{\Psi}_{ASNP}(i,j)$ restricted to the

$$\text{NPAC region} \qquad \text{90E to 270E and 10N to 60N} \tag{8}$$

$$\text{and to the ASNP region} \qquad \text{0E to 160E and 5N to 50N.} \tag{9}$$

We used a Hamming-window for the restrictions. The squared local projection amplitudes $a_{k,NPAC}^2(i,j) = (\mathbf{\Psi}_{NPAC}(i,j), \mathbf{s}_k(96,j))_E^2$ for SVs at $t = 96$h and $b_{k,ASNP}^2(i,j) = (\mathbf{\Psi}_{ASNP}(i,j), \mathbf{s}_k(0,j))_E^2$ for SVs at $t = 0$h give fractions of kinetic energy in the NPAC and the Asia - North Pacific region, where the SVs $\mathbf{s}_k(96,j)$ and $\mathbf{s}_k(0,j)$ occur. The amplitudes $a_{k,l,NPAC}(i,j)$ and $b_{k,l,ASNP}(i,j)$ are defined accordingly.

The fractions of kinetic energy explained by the NPAC wave train is then given by

$$\begin{aligned} E_{96,l}(i,j) &= \frac{1}{\overline{E_{NPAC}}}(a_{1,l,NPAC}^2(i,j) + a_{2,l,NPAC}^2(i,j)), \\ \text{and} \qquad E_{0,l}(i,j) &= \frac{1}{\overline{E_{ASNP}}}(b_{1,l,ASNP}^2(i,j) + b_{2,l,ASNP}^2(i,j)) \end{aligned} \tag{10}$$

The energies $E_{NPAC}(i,j)$ and $E_{ASNP}(i,j)$ are defined as in eq.7.

The observed growth $\sigma_{obs,l,m}^2(i,j)$ of the NPAC mode depends also on the time lag $\Delta t = m$ h between the time serieses. Here m has to be a multiple of 24 because we used daily data.

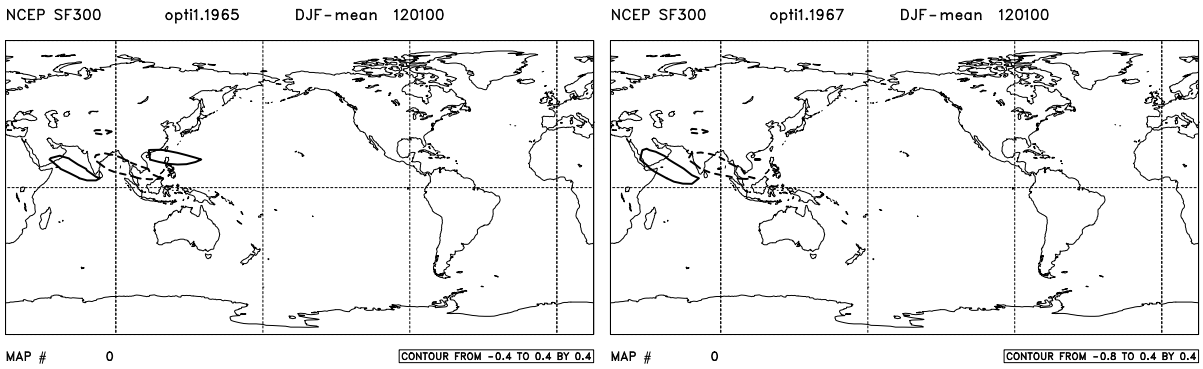

Figure 1: First SV $\mathbf{s}_1(t,j)$ for DJF basic flow $j = 65$ and $j = 67$ and optimization time $t_{opt} = 96$h at development time $t = 0h$.

The observed growth is given by the quotient of explained kinetic energies at optimization and at initial time:

$$\sigma^2_{obs,l,m}(i,j) = \frac{E_{96,l}(i - m/24, j)}{E_{0,l}(i,j)} \tag{11}$$

In all cases, in which the seasons l and j are equal, the index l is omitted

3 Results

Analyzing the relevance of SVs for teleconnections we concentrate on SVs with large eigenvalues. If not given else, the results presented are for the optimization time $t_{opt} = 96$h.

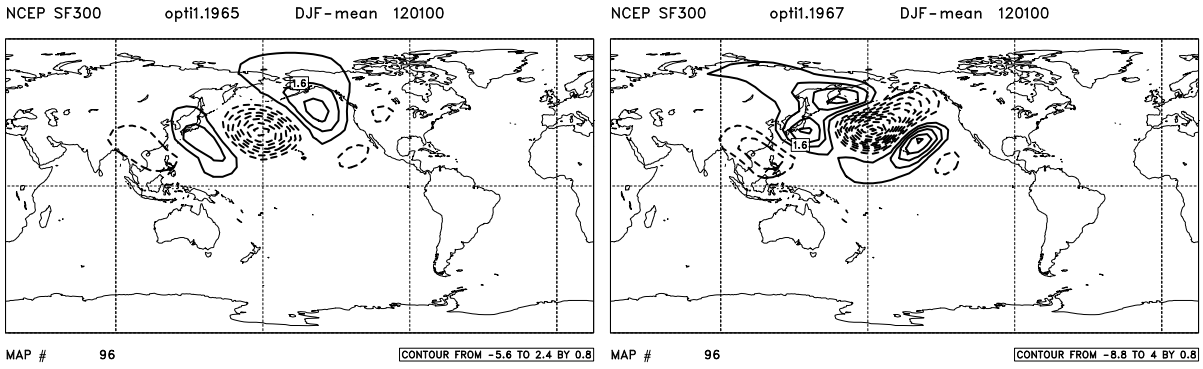

Figure 2: As Fig.1 but at development time $t = 96h$.

3.1 Characteristics of Singular Vectors

Fig. 1 and 2 show the SV $s_1(t,65)$ and $s_1(t,67)$ for $t = 0$h and $t = 96$h. The shapes of the leading SVs at $t = 96$h remind on a local Rossby wave packet with wave number 5 to 6. The group velocity and propagation path are consistent with Rossby wave packet theory (*Buizza and Palmer*, 1995; *Hoskins et al.*, 2000). The second SVs have shapes very similar to those of the leading SVs, but show phase shifts of $\pi/2$ in direction of the SVs propagation (*Li and*

Ji, 1997). In all seasons $j = 58$ to $j = 97$ the eigenvalues of the first two SVs are close to another, e.g. $\sigma_1^2(65) = 11.9$ and $\sigma_2^2(65) = 10.1$ or $\sigma_1^2(67) = 28.4$ and $\sigma_2^2(67) = 24.9$. As shown in Fig. 3 the leading eigenvalues range from 10 to 30. The first SV of each year has a shape similar to those shown in Fig.1 and 2. We call a pair of SVs 1 and 2 "NPAC mode".

In all seasons considered there appear just six other pairs of SVs with properties comparable to the NPAC modes but with different locations. The other SVs (out of 480 for each basic flow) do not develop a growing, localized, propagating wave packet with a decreasing, dominant wave number. The SVs $\mathbf{s}_3(t, 65)$ and $\mathbf{s}_5(t, 65)$ are the components of the second RWT mode. We name it East Pacific-North Atlantic (EPNA) mode. Similar SVs uniquely identifiable as the EPNA mode occur in a few northern winter SV bases only. The remaining 5 RWT modes found are the Central Pacific (CPAC), Tropical Pacific-North Atlantic (TPNA), Tropical Atlantic-West Pacific (TAWP), South Pacific (SPAC), and South Atlantic-Indian Ocean (SAIO) modes.[1]

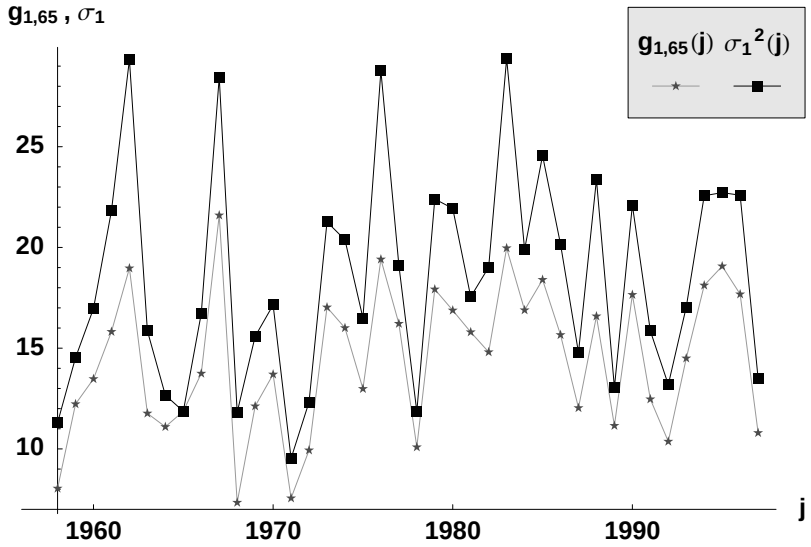

Figure 3: eigenvalues $\sigma_1^2(j)$ and growth factors $g_{1,65}(j)$ of SV $\mathbf{r}_1(0, 65)$.

The appearance of the RWT modes in some regions on the globe only is consistent with the results of *Buizza and Palmer* (1995). Interestingly the shapes and propagation paths of these modes are rather insensitive to changes of the basic flow. This can be seen clearly from Fig.4. It shows the centers of location[2] for RWT modes NPAC, CPAC and EPNA of season $l = 65$ developing in basic flows of all other seasons $j = 58$ to $j = 97$ for development times $t = 0$ to $t = 96$h. The paths spread much more for times $t > 96$h, for which the RWT modes energy is dissipating. The corresponding growth factors $g_{k,l}(j)$ change significantly. This is shown by the gray line in Fig.3 for the first SV.

The growth factors can be compared with the eigenvalues for the NPAC mode only. The gray line in Fig. 3 shows the growth factors $g_{1,65}(j)$ in comparison to $\sigma_1^2(j)$ as a function of the season j. It can be seen, that the values of $g_{1,65}(j)$ are smaller than those of $\sigma_1^2(j)$, except for the year $j = 65$, where both values have to be equal [see (4)]. The correlation of the time serieses ($= 0.95$) justifies the relevance of the quantity $g_{k,l}(j)$ introduced.

[1]Examples are given on the homepage www.uni-lepzig.de/ meteo/AWILL/anima.html.

[2]The centers of location are given by the location of the maxima of Gaussian envelopes. The parameters of the envelopes are calculated as least square fits to the kinetic energy of the wave trains.

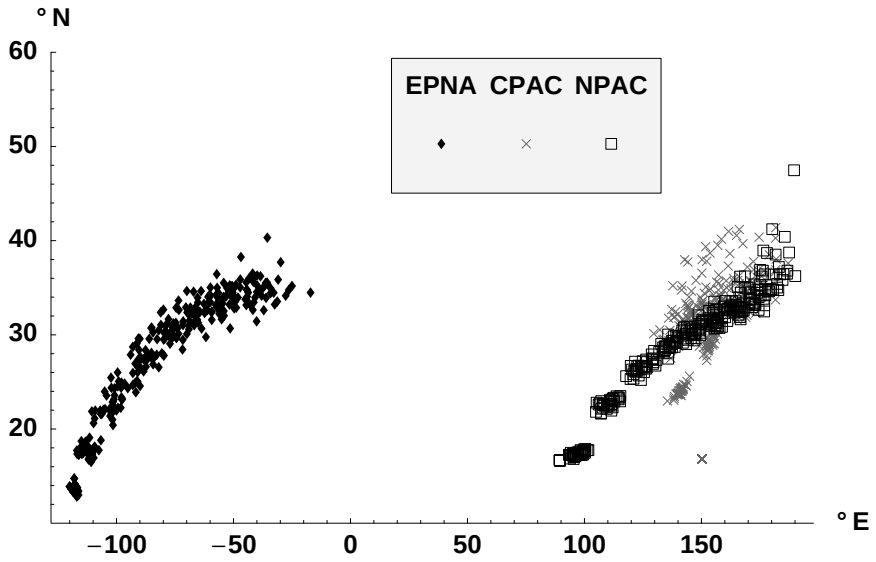

Figure 4: Centers of location of $\mathbf{s}_{k,65}(t_{opt}, j)$ at development times 0 (in subtropics) to 96h (in mid latitudes) (in 12h steps) for k equal to 1,3 and 7, which are the first components of the north hemispheric wave trains NPAC, CPAC and EPNA.

A comparison of $\mathbf{s}_1(96, 67)$ with $\mathbf{s}_{1,65}(96, 67)$ provides further evidence for the similarity between the shapes of SV $\mathbf{s}_1(t, j)$ and $\mathbf{s}_{1,65}(t, j)$ in the basic state flow of year j. The SV $\mathbf{s}_1(96, 67)$ ($\sigma_1^2(67) = 28.4$) gives an example of a leading SV with a high eigenvalue. The SV $\mathbf{s}_1(96, 65)$ is very typical and similar to the corresponding SVs of a climatological basic flow $\overline{\mathbf{\Psi}}$ and also to the leading SVs presented by *Li and Ji* (1997). Consistently, a SV very similar to $\mathbf{s}_1(96, 67)$ was also obtained calculating $\mathbf{s}_{1,65}(96, 67)$. Further inspection of the SVs shows the appearance of only one other RWT mode for climatological basic flows: the first component of the EPNA mode appears as 12th SV if no forcing is applied and as 7th SV by *Li and Ji*.

Features of seasonal basic flows (smoothed out in climatological flows) seem to be responsible for the appearance of additional RWT modes and dominate the strength and the development of the shape of the RWT modes in the growth phase, and not the initial conditions.

3.2 Singular Vectors and Observations

As shown by *Borges and Sardeshmukh* (1995) structures similar to the NPAC mode shown in Fig.2 are found in observations. However, it is unclear whether the finite time instability is the reason for the high projection amplitudes found. *Sardeshmukh et al.* (1997) analysed the relevance of SVs in atmospheric dynamics and showed, that using a climatological basic flow the SVs of an unforced, damped barotropic model can not explain the tendency of global kinetic energy over some days.
However, there has not to be any relation between the time series of the kinetic energy on the globe and in a specific region. Therefore parts of synoptic dynamics may be described by RWT modes of an unforced barotropic model, if their development is dominated by the basic flow and not nonlinear processes, forcing and dissipation. The features of the SVs discussed in the previous section indicate, this might be the case at least for the NPAC mode. The occurence of the components of the NPAC mode in the SV basis of each season gives us the opportunity to compare the time serieses of eigen values $\sigma_1^2(j)$ with that of the observed

growth of the NPAC mode $\sigma^2_{obs,m}(i,j)$ (eq.11).

Further investigating the relevance of SVs for teleconnections we begin the analysis of the observed space-time structure of SVs with a calculation of the occurence of SVs in observations. Because the eigenvalues $\sigma^2_k(j)$ change significantly from year to year (see Fig.3), the components of a particular RWT mode may have different ranking in different seasons. Since we are interested in interannual variability of RWT modes and not in the variability of a SV with a specific ordering number (but arbitrary structure), we look at the time series of growth factors $g_{k,l}(j)$ introduced in section 2, which is uniquely related to a specific SV.

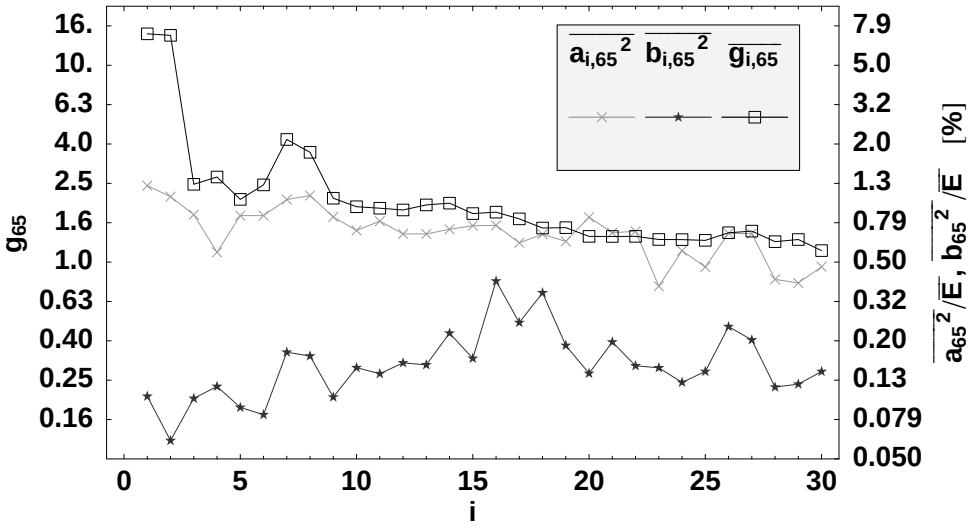

Figure 5: Climatologically averaged growth factors $\overline{g_{k,65}}$ and squared projection amplitudes $\overline{a^2_{i,65}}$ and $\overline{b^2_{i,65}}$.

We calculated the projection amplitudes $a_1(i,j)$, $b_1(i,j)$ and $a_{k,l}(i,j), b_{k,l}(i,j)$ for different basis years l (see eq.5 and 6). Figure 5 shows the climatological average of the growth factors $\overline{g_{k,65}}$ in comparison to that of the squared projection amplitudes $\overline{a^2_{k,65}}(i,j)$ and $\overline{b^2_{k,65}}(i,j)$ at optimization and initial time respectively for the SVs 1 to 30. The peak for $k=7$ and $k=8$ in $\overline{g_{k,65}}(j)$ is due to relatively high growth factors of $\mathbf{s}_7(0,65)$ and $\mathbf{s}_8(0,65)$ in other basic flows. The expectation value for $a^2_{k,l}(i,j)/\overline{E}$ and $b^2_{k,l}(i,j)/\overline{E}$ is $100/480\% \simeq 0.2\%$. A comparison of the curves reveals that only fully developed SVs (at $t=t_{opt}$) with large growth factors have large projection amplitudes. Among the first 30 SVs of season $l=65$ there are several RWT mode components (e.g. $k=1,2,3,5,7$ and 8). Since they are more localized than other SVs, we asked, which SVs are dominant in which region. We defined different regions with nearly equal area. We found remarkably high projection amplitudes for RWT mode components at $t=t_{opt}$ and for maximaly decaying SVs (which have shapes at initial time similar to those of RWT modes at optimization time) at $t=0$ (not shown).

Let us now focus on the NPAC mode, which corresponds to $s_1(t,j)$ and $s_2(t,j)$ for all years j. Fig.6 shows the fractions of kinetic energy in the appropriate region explained by the NPAC mode ($E_0(i,j)$ and $E_{96}(i,j)$ defined in 10) for 270 days of seasons $j=65$ to $j=67$. It is remarkable that the fully developed NPAC mode explains up to 60 % of the climatological average of the kinetic energy in the region of occurrence. A strong variability of E_{96} can be observed around the average value $\overline{E}_{96}=12.4\%$. In contrast, the energy fraction E_0 has the order of the statistical expectation value of 1.3%, as shown by the curve $E_0(t)$. Remarkably,

the seasonally averaged energy $\tilde{E}_{96}(j)$ is correlated with the singular values $\sigma_1^2(j)$ and $\sigma_2^2(j)$ ($c_{\sigma_1^2,\tilde{E}_{96}} = 0.46$). Assuming 40 independent random values, the probability is 99 % that the correlation threshold $c_{th99} = 0.37$ will not be exceeded (*Storch and Zwiers*, 1999, ch.8.2.3).

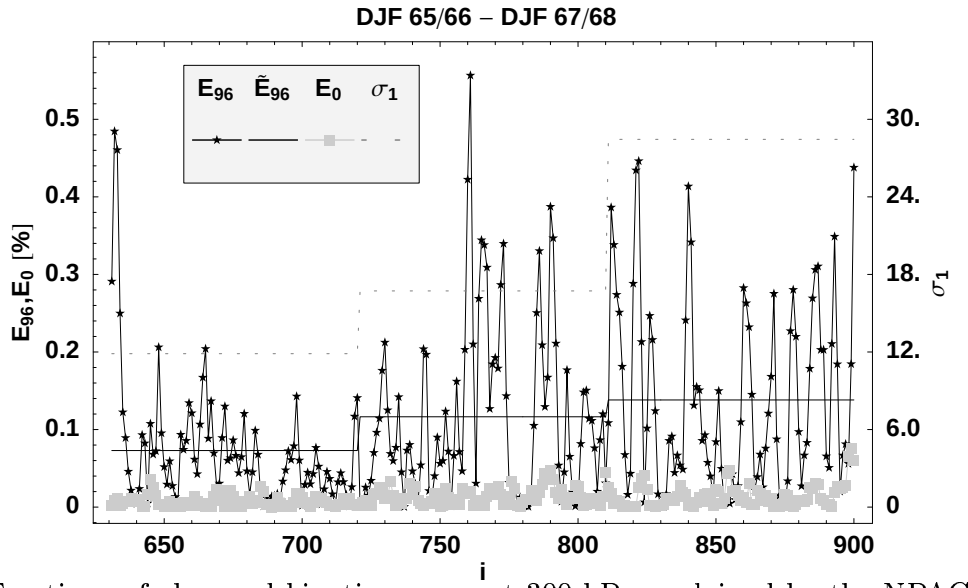

Figure 6: Fractions of observed kinetic energy at 300 hPa explained by the NPAC modes at development times $t = 0$h in the NSAP and at $t = 96$h in the NPAC region on 270 days of the DJF seasons 65/66 ($j = 65$) to 67/68 ($j = 67$).

The projection amplitudes for the 3600 days in 40 seasons, in parts presented in Fig.6, were used to calculate the observed time lag Δt between $E_0(i,j)$ and $E_{96}(i,j)$ and the observed growth factors $\sigma_{obs,l,m}(i,j)$ (eq.11). The left picture in Fig.7 shows a significant correlation maximum ($c_{max} = 0.142$, $c_{th99} = 0.04$) between $E_0(i,j)$ and $E_{96}(i,j)$ for the time lag of 72h. Regarding that the observed projection amplitudes $E_0(i,j)$ of the SVs at initial time are nearly 0.8% of the climatological kinetic energy $\overline{E_{ASNP}}$ which is much smaller than the physical precision of analysed data ($\simeq$ 3% of the averaged values) and that the distance between subsequent dates is 24h, the result can be seen consistent with the optimization time $t_{opt} = 96$h, for which the correlation is found to be 0.09.

The right picture in Fig.7 shows the dependency of the eigenvalues $\sigma_1^2(j)$ and the seasonally averaged observed growth factors $\widetilde{\sigma^2_{obs,96}}(j)$, assuming a time lag $\Delta t = 96$h. The dependency for $\Delta t = 72$h is very similar. The regression line $f(\sigma) = 0.2 + 1.0\sigma$ is calculated as a two side least square fit. It is consistent with the theoretical line $f_t(\sigma) = \sigma$. The correlation coefficient between $\sigma_1^2(j)$ and $\widetilde{\sigma^2_{obs,96}}(j)$ was found to be 0.41 ($c_{th99} = 0.37$).

3.3 Singular Vectors and Teleconnections

The high spatial localisation of propagation paths makes the SVs a possible link between weather and climate time scales. The results of the previous section provide evidence for the dynamical relevance of the NPAC mode in atmospheric dynamics. In this region the PNA occurs. It appears obvious to try to connect both.

The PNA-Index as defined by *Wallace and Gutzler* (1981) reflects large scale variability of atmospheric fields. We therefore compare it with the energy explained by the NPAC mode at optimization time. Fig.8 shows the seasonally averaged time series of the kinetic energy

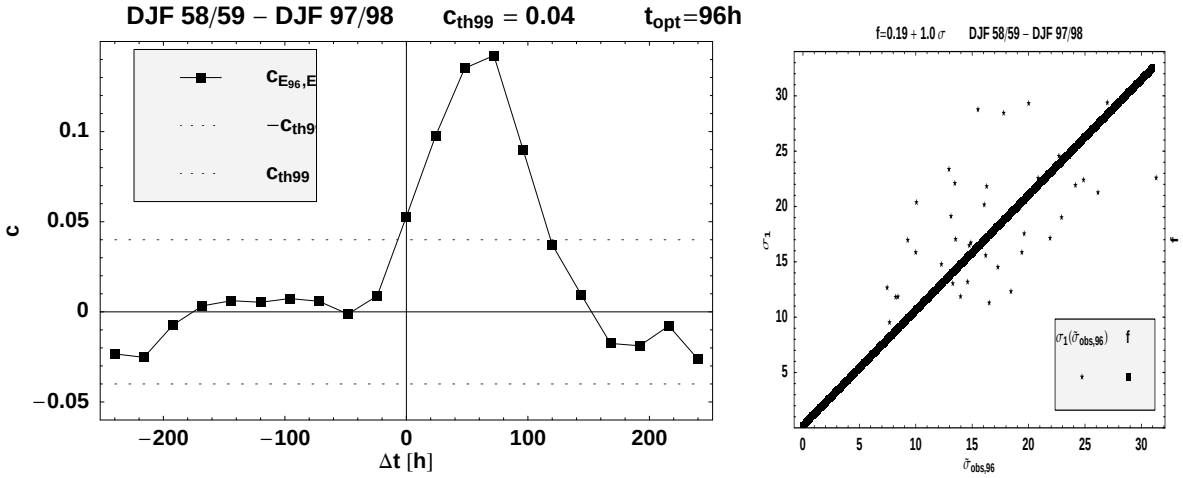

Figure 7: Observed growth factors.

$\widetilde{E_{96}(j)}$ explained by the NPAC mode (see also Fig. 6) and of the kinetic energy $\widetilde{E_{96,67}}$ explained by the NPAC mode of season $j = 67$. The third line shows the seasonally averaged PNA-Index ($\widetilde{PNA - I}$). The correlation coefficient $c_{\widetilde{E_{96}},\widetilde{PNA-I}} = 0.3$ ($c_{th95} = 0.26$) is above the 95% significancy threshold. Surprisingly the correlation $c_{\widetilde{E_{96,67}},\widetilde{PNA-I}} = 0.52$ between the projection on the NPAC mode of season $j = 67$ and the PNA-Index is remarkably high. The correlations $c_{\widetilde{E_{96,l}},\widetilde{PNA-I}}$ between the seasonal energy expained by the NPAC modes of different seasons l and the PNA-Index range between 0.2 and 0.6 and provide relatively high values for seasons with high eigenvalues (e.g. $\sigma_1^2(67) = 28.4$).

However, the leading SV at $t = 96$h is located in the North Pacific region, while the PNA is found 30° to 50° further east. We investigated also SVs for longer development and optimization times. No remarkable correlation could be found between explained energy and PNA-Index for SVs at times around $t = t_{opt} = 144h$.

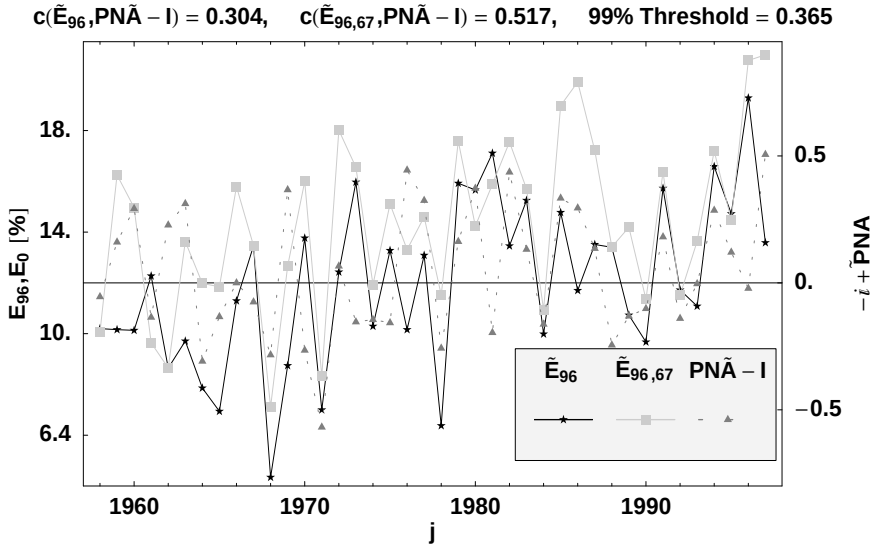

Figure 8: DJF averaged PNA-Index and DJF averaged fraction of explained kinetic energy by NPAC wave trains (see Eq.10).

4 Summary and Conclusions

We investigated RWT modes, given as Rossby wave train like SVs of an unforced, damped, barotropic model. The results indicate, that their development is dominated by the basic flow in the growth phase of 96h.

In all 40 seasonal basic flows considered seven RWT modes could be found. Only two RWT modes can be found in forced (*Li and Ji*, 1997) and unforced SVs of climatological basic flows. Interestingly, the shapes and propagation paths of the RWT modes identified are remarkably constant. This makes them a reasonable candidate to connect the time scales of weather and climate and the finite time instability a possible mechanism for organizing teleconnections.

Remarkably, the fractions of kinetic energy explained by the fully developed ($t = t_{opt}$) components of the RWT modes in observed 300hPa streamfunction data are large (up to 60% of the climatological kinetic energy in each region). On the other hand, marginally growing or decaying SVs, SVs without a RWT mode structure, or SVs at $t = 0$ explain only small fractions of energy. This indicates that all fully developed RWT modes exhibit spatial structures which are well observed in the atmosphere.

The RWT mode with highest energy growth is the NPAC mode, which components are the leading SVs for each of the seasonal basic flows. This gave us the opportunity to compare the space-time structure of the calculated and of the observed NPAC mode. We found the observed time lag of the NPAC mode to be consistent with the time lag of 96h (optimization time) assumed in the calculation of the SVs. Furthermore, we found the observed energy growth of the NPAC mode to have nearly the same expectation value as and to be significantly correlated with the eigenvalues. This indicates, that finite time instability is able to describe important features of the observed NPAC modes structure.

Finally, we investigated the suggested relevance of the NPAC mode for the PNA teleconnection. Indeed, we found a weakly significant correlation (c=0.3) between the time series of the fraction of kinetic energy $\widetilde{E_{t_{opt}}(j)}$ explained by the NPAC mode and the time series of the PNA-Index $\widetilde{PNA - I(j)}$. Interestingly, we found a significant correlation of 0.52 for the energy explained by the strongly growing NPAC mode of season 67/68 ($\widetilde{E_{t_{opt}}(j)}$) and no significant corrrelation using projections on SVs for longer optimization times (e.g. $t_{opt} = 144$h).

During the growth phase of 96h the dynamics of the NPAC mode seems to be dominated by the basic flow. Beyond this time other processes become dominant (nonlinearity, forcing and dissipation). We found a spread of propagation paths, changes in shape and no correlation with the PNA-Index.

The results give further evidence for the importance of finite time instability for atmospheric dynamics on timescales beyond the weather and give some hints for a possible connection between SVs and the dynamics of teleconnections. An explanation of the PNA seems not to be possible in the framework of a damped, unforced barotropic model.

Acknowledgements: We wish to thank Dr.H.Heinrich for providing the numerical scheme for SV analysis and Mr.F.Senf for processing of the projection amplitudes. This work was supported by the German Climate Research Program (DEKLIM).

References

Borges, M. D., and P. D. Sardeshmukh, Barotropic Rossby Wave Dynamics of Zonally Varying Upper-Level Flows During Northern Winter, *J.Atmos.Sci.*, *52*, 3779–3796, 1995.

Branstator, G., Circumglobal Teleconnections, the Jet Stream Waveguide, and the North Atlantic Oscillation, *J.Clim.*, *15*, 1893–1910, 2002.

Buizza, R., and T. Palmer, The Singular-Vector Structure of the Atmospheric Global Circulation, *J.Atmos.Sci.*, *52*, 1434–1456, 1995.

Goodman, J. C., and J. Marshall, Using Neutral Vectors to Study Low-Frequency Atmospheric Variability, *J.Atmos.Sci.*, *59*, 3206–3222, 2002.

Heinrich, H., Optimal wachsende Störungen in einem barotropen Modell, Diplomarbeit, LIM, Institut für Meteorologie der Universität Leipzig, Stephanstr.3, 04107 Leipzig, 1999.

Hoskins, B., R. Buizza, and J. Badger, The Nature of Singular Vector Growth and Structure, *QJR Meteorol.Soc.*, *126*, 1565–1580, 2000.

Hoskins, B. J., and T. Ambrizzi, Stationary Rossby-Wave Propagation in a Baroclinic Atmosphere, *QJR Meteorol.Soc.*, *123*, 919–928, 1997.

Hoskins, B. J., and D. J. Karoly, The Steady Linear Response of a Spherical Atmosphere to Thermal and Orographic Forcing, *J.Atmos.Sci.*, *38*, 1179–1196, 1981.

Kalnay, E., et al., The ncep/ncar 40-year reanalysis project, *Bulletin of the American Meteorological Society*, *77*, 437–471, 1996.

Lau, N.-C., The Observed Structure of Tropospheric Stationary Waves and the Local Balance of Vorticity and Heat, *J.Atmos.Sci.*, *36*, 996–1016, 1979.

Li, Z., and L. Ji, Efficient Forcing and Atmospheric Teleconnections, *QJR Meteorol.Soc.*, *123*, 2401–2423, 1997.

Metz, W., Singular Modes and Low-Frequency Atmospheric Variability, *J.Atmos.Sci.*, *51*, 1740–1753, 1994.

Navarra, A., Teleconnection Patterns, in *Analysis of Climate Variability*, edited by H. V. Storch and A. Navarra, pp. 215–225, Springer-Verlag, 1995.

Sardeshmukh, P. D., M. Newman, and M. D. Borges, Free Barotropic Rossby Wave Dynamics of the Wintertime Low-Frequency Flow, *J.Atmos.Sci.*, *54*, 5–23, 1997.

Simmons, A. J., J. M. Wallace, and G. W. Branstator, Barotropic Wave Propagation and Instability, and Atmospheric Teleconnection Patterns, *J. Atmos. Sci.*, *40*, 1363–1392, 1983.

Storch, H. V., and F. W. Zwiers, *Statistical Analysis in Climate Research*, Cambridge University Press, 1999.

Wallace, J. M., and D. S. Gutzler, Teleconnections in Geopotential Heigh Field During the Northern Hemisphere Winter, *Mon. Wea. Rev.*, *109*, 784–812, 1981.